Signal Processing 143 (2018) 134–139

Contents lists available at ScienceDirect

Signal Processing

journal homepage: www.elsevier.com/locate/sigpro

Short communication

Classification and localization of mixed near-field and far-field sources using mixed-order statistics☆

Zhi Zheng*, Jie Sun, Wen-Qin Wang, Haifen Yang

School of Communication and Information Engineering, University of Electronic Science and Technology of China, Chengdu 611731, China

ARTICLE INFO

Article history:
Received 23 July 2017
Revised 27 August 2017
Accepted 31 August 2017
Available online 1 September 2017

Keywords:
Mixed sources
Source localization
Near-field
Far-field
Fourth-order cumulant

ABSTRACT

In this paper, a novel algorithm based on mixed-order statistics is proposed for mixed near-field and far-field source localization. Firstly, the direction-of-arrivals (DOAs) of far-field signals are estimated using the conventional MUSIC method based on second-order statistics. Then, a special fourth-order cumulant matrix of the array output is constructed, which is only related to DOA parameters of mixed sources. After estimating the kurtosis of far-field signals, the related far-field components can be removed from the constructed cumulant matrix and the near-field components can be derived. With the near-field data in the cumulant domain, the DOA estimations of near-field sources can be performed using high-order MUSIC spectrum. Finally, with the near-field DOA estimates, the range parameters of near-field sources can be obtained via one-dimensional search. The proposed algorithm involves neither two-dimensional search nor additional parameter pairing processing. Moreover, it can achieve a more reasonable classification of the source types. Simulations results demonstrate the advantages of the proposed algorithm in comparison to the existing methods.

1. Introduction

Source localization is an important topic in many array processing applications such as radar, sonar, wireless communications, electronic surveillance and seismic exploration [1–4]. In the past few decades, it has received considerable attention, and various high-resolution algorithms like MUSIC [5] and ESPRIT [6] have been developed to perform the direction-of-arrival (DOA) estimation of far-field (FF) sources under the plane waves hypothesis. In the near-field (NF) sources scenario, both DOA and range parameters should be estimated since the plane waves assumption is not valid, and some near-field localization algorithms [7–20] are also available. However, in some practical applications, both near-field and far-field sources may coexist, such as speaker localization using microphone arrays. In the mixed sources scenario, the aforementioned algorithms may fail to localize the mixed sources.

To cope with this issue, some algorithms have been recently presented. Based on two special comulant matrices of array outputs, Liang et al. [21] presented a two-stage MUSIC (TSMUSIC) algorithm to deal with the problem of mixed near-field and far-field source localization. However, the TSMUSIC algorithm is based on high-order statistics (HOS) and thus it is computationally inefficient and can not deal with Gaussian sources. Motivated by the above drawback, He et al. [22] developed the MBODS method based on second-order statistics (SOS). The MBODS method can correctly distinguish the types of sources and avoid both two-dimensional (2-D) search and high-order statistics calculations. However, when locating the near-field sources, the MBODS method suffers from partial aperture loss, reducing the accuracy to some extent. Later, Liu et al. [23] presented another SOS-based method for mixed far-field and near-field source localization. Compared with the MBODS method, the method of Liu and Sun [23] can achieve a more reasonable classification of the signal types, reduce the aperture loss, as well as enhance the localization accuracy of near-field sources. Resorting to a special sparse array geometry, Wang et al. [24] presented a mixed-order MUSIC algorithm, which has improved the accuracy and resolution of mixed source localization. Using the ESPRIT-Like and polynomial rooting methods, Jiang et al. [25] presented a new algorithm for mixed source localization. The method of Jiang et al. [25] not only offers better performance for both the DOA and range estimations, but also requires less computational cost than the algorithms of Liang and co-workers [21,22]. Wang et al. [26] adopted the sparse reconstruction technique to locate mixed sources, which has some salient advantages in resolution and accuracy over the subspace-based techniques. However, the sparse reconstruction method [26] will meet with some performance deterioration under unknown the number

☆ Fully documented templates are available in the elsarticle package on CTAN.

* Corresponding author.
E-mail addresses: zz@uestc.edu.cn (Z. Zheng), sunj@std.uestc.edu.cn (J. Sun), wqwang@uestc.edu.cn (W.-Q. Wang), yanghf@uestc.edu.cn (H. Yang).

http://dx.doi.org/10.1016/j.sigpro.2017.08.025
0165-1684/

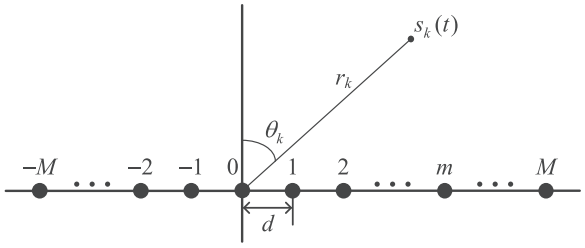

Fig. 1. Uniform linear array configuration.

of sources. To overcome the shortcoming, Tian et al. [27] proposed a mixed source localization algorithm using the sparse representation of two special cumulant vectors. Liu et al. [28] propose an ESPRIT method for localization of mixed far-field and near-field cyclostationary sources. The ESPRIT algorithm can greatly reduce the computational cost and achieve automatic pairing of the DOA and range estimates. Wang et al. [29] proposed another low-complexity algorithm using array partition and high-order cumulants, which can alleviate the array aperture loss and avoid spectral search. By taking advantage of the differences between the far-field and the near-field covariance matrices, the spatial differencing algorithms of Liu and Sun [30,31] are presented for mixed source classification and localization. Compared with the previous techniques, the spatial differencing methods can not only achieve a more reasonable classification of the source types, but also provide higher estimation accuracy.

In this paper, we propose a novel algorithm for mixed source localization based on second-order and fourth-order statistics. The proposed algorithm is implemented by three stages: (i) The DOAs of far-field sources are estimated by the conventional MUSIC method. (ii) A fourth-order cumulant matrix containing only DOA information of sources is constructed. After estimating the kurtosis of far-field signals, the related far-field components can be removed from the constructed cumulant matrix and the near-field components are obtained. With the near-field components in cumulant domain, the DOAs of near-field sources can be obtained using high-order MUSIC spectrum. (iii) With the near-field DOA estimates, the range parameters of near-field sources are obtained by one-dimensional (1-D) search. Our approach requires neither 2-D search nor extra parameter pairing processing, and it can realize a more reasonable classification of the signals types. Its superiorities over the traditional methods are verified by simulation results.

The rest of this paper is organized as follows. The received signal model of mixed sources along with some basic assumptions are described in Section 2. A novel approach for mixed source classification and localization is proposed in Section 3. Simulations and results are provided in Section 4. Finally, conclusions are drawn in Section 5.

2. Signal model and basic assumptions

Consider K (near-field or far-field) narrowband sources impinging on a symmetric uniform linear array with $2M+1$ elements and inter-element spacing d, as depicted in Fig. 1. Let the array center be the phase reference point, the signal received by the mth sensor can be expressed as

$$y_m(t) = \sum_{k=1}^{K} s_k(t) e^{j\tau_{mk}} + n_m(t) \tag{1}$$

where $s_k(t)$ is the kth signal waveform, $n_m(t)$ denotes the mth sensor noise, and τ_{mk} represents the propagation time of the kth source between the 0th and mth sensor. When the kth source is a near-field one, τ_{mk} is given by

$$\tau_{mk} = m\omega_k + m^2\phi_k \tag{2}$$

where ω_k, ϕ_k have the following forms:

$$\omega_k = -2\pi \frac{d}{\lambda} \sin\theta_k, \tag{3}$$

$$\phi_k = \pi \frac{d^2}{\lambda r_k} \cos^2\theta_k \tag{4}$$

where λ is the wavelength of the incoming signal. θ_k and r_k denote the DOA and range of the kth source at the phase origin, respectively. Otherwise, when the kth source is located in the far-field region, the range parameter is $r_k \to \infty$, and the associated parameter ϕ_k is approximately equal to zero. Then τ_{mk} can be expressed as

$$\tau_{mk} = m\omega_k. \tag{5}$$

In matrix form, (1) can be written as

$$\mathbf{y}(t) = \mathbf{A}_N\mathbf{s}_N(t) + \mathbf{A}_F\mathbf{s}_F(t) + \mathbf{n}(t) \tag{6}$$

where $\mathbf{y}(t)$ and $\mathbf{n}(t)$ are $(2M+1)\times 1$ complex vectors, and

$$\mathbf{y}(t) = [y_{-M}(t), \ldots, y_0(t), \ldots, y_M(t)]^T \tag{7}$$

$$\mathbf{A}_N = [\mathbf{a}(\theta_1, r_1), \ldots, \mathbf{a}(\theta_{K_1}, r_{K_1})] \tag{8}$$

$$\mathbf{A}_F = [\mathbf{a}(\theta_{K_1+1}), \ldots, \mathbf{a}(\theta_K)] \tag{9}$$

$$\mathbf{s}_N(t) = [s_1(t), \ldots, s_{K_1}(t)]^T \tag{10}$$

$$\mathbf{s}_F(t) = [s_{K_1+1}(t), \ldots, s_K(t)]^T \tag{11}$$

$$\mathbf{n}(t) = [n_{-M}(t), \ldots, n_0(t), \ldots, n_M(t)]^T \tag{12}$$

where

$$\mathbf{a}(\theta_k, r_k) = \left[e^{j(-M\omega_k + M^2\phi_k)}, \ \ldots, 1, \ldots, \right. \\ \left. e^{j(M\omega_k + M^2\phi_k)}\right]^T \tag{13}$$

denotes the $(2M+1)\times 1$ steering vector, and the superscript T denotes the transpose. It is worth mentioning that in signal model (6), the first K_1 sources are assumed to be near-field sources and the remaining $(K-K_1)$ are far-field sources.

Throughout this paper, the following assumptions are required to hold:

1. The source signals are statistically independent, zero-mean random processes with nonzero kurtosis, and all signals impinge on the receiver array from distinct directions.
2. The sensor noise is the additive spatially white Gaussian one with zero-mean, and independent of the source signals.
3. The sensor array is a ULA with inter-element spacing $d = \lambda/4$, and the source number is less than the number of elements, namely, $K < 2M+1$.

3. Proposed algorithm

3.1. DOA estimations of far-field sources

According to (6), we can obtain the covariance matrix of the array received data $\mathbf{y}(t)$ as

$$\mathbf{R} = E\{\mathbf{y}(t)\mathbf{y}^H(t)\} \tag{14}$$

where the superscript H stands for the conjugate transpose, and $E\{\cdot\}$ denotes the statistical expectation.

Assume that the source number K is known or accurately estimated by the information theoretic criteria [32]. The eigenvalue decomposition (EVD) of $\mathbf{R}$ yields

$$\mathbf{R} = \mathbf{U}_s \mathbf{\Sigma}_s \mathbf{U}_s^H + \mathbf{U}_n \mathbf{\Sigma}_n \mathbf{U}_n^H \tag{15}$$

where $\mathbf{\Sigma}_s$ is the $K \times K$ diagonal matrix containing the K largest eigenvalues of $\mathbf{R}$, and $\mathbf{U}_s$ is the $(2M+1) \times K$ signal-subspace matrix spanned by the eigenvectors corresponding to the K largest eigenvalues. $\mathbf{\Sigma}_n$ is the $(2M+1-K) \times (2M+1-K)$ diagonal matrix containing the $2M+1-K$ smallest eigenvalues of $\mathbf{R}$, and $\mathbf{U}_n$ is the $(2M+1) \times (2M+1-K)$ noise-subspace matrix spanned by the eigenvectors associated with the $2M+1-K$ smallest eigenvalues.

Then, we can create the following 2-D MUSIC spectral function:

$$f(\theta, r) = \left[\mathbf{a}^H(\theta, r)\mathbf{U}_n\mathbf{U}_n^H\mathbf{a}(\theta, r)\right]^{-1} \tag{16}$$

where the search domain for DOAs is $\theta \in [-\pi/2, \pi/2]$, and the search domain for ranges is the Fresnel region [14] plus $r = \infty$. The 2-D spatial spectrum of (16) will exhibit exactly K peaks [7], of which the peaks located at $\{\theta = \theta_k, r = \infty\}$ $(k = K_1 + 1, \ldots, K)$ correspond to $K - K_1$ far-field sources.

That is, the DOAs of far-field sources can be found by looking for the $K - K_1$ peaks from the following DOA spectrum [22]:

$$P_F(\theta) = \left[\mathbf{a}^H(\theta, \infty)\mathbf{U}_n\mathbf{U}_n^H\mathbf{a}(\theta, \infty)\right]^{-1}. \tag{17}$$

3.2. Source classification and DOA estimations of near-field sources

Based on the assumptions, we define the fourth-order cumulant of the array outputs as

$$\begin{aligned}
&\mathrm{cum}\{y_m(t), y_n^*(t), y_p^*(t), y_q(t)\} \\
&= \mathrm{cum}\left\{\sum_{k=1}^{K} s_k(t)e^{j(m\omega_k+m^2\phi_k)}, \left(\sum_{k=1}^{K} s_k(t)e^{j(n\omega_k+n^2\phi_k)}\right)^*,\right. \\
&\left.\left(\sum_{k=1}^{K} s_k(t)e^{j(p\omega_k+p^2\phi_k)}\right)^*, \sum_{k=1}^{K} s_k(t)e^{j(q\omega_k+q^2\phi_k)}\right\} \\
&= \sum_{k=1}^{K} e^{j\{[(m-n)-(p-q)]\omega_k+[(m^2-n^2)-(p^2-q^2)]\phi_k\}} \\
&\quad \times \mathrm{cum}\{s_k(t), s_k^*(t), s_k^*(t), s_k(t)\} \\
&= \sum_{k=1}^{K} c_{4,s_k} e^{j\{[(m-n)-(p-q)]\omega_k+[(m^2-n^2)-(p^2-q^2)]\phi_k\}}
\end{aligned} \tag{18}$$

where $c_{4,s_k} = \mathrm{cum}\{s_k(t), s_k^*(t), s_k^*(t), s_k(t)\}$ is the kurtosis of the kth signal, $m, n, p, q \in [-M, M]$, and the superscript * denotes the complex conjugate.

To retain the ω_k term and remove the ϕ_k term in (18), both $(m-n)-(p-q) \neq 0$ and $(m^2-n^2)-(p^2-q^2) = 0$ are required. For simplicity, we assume $n = -m$ and $q = -p$. Then, (18) becomes

$$\begin{aligned}
&\mathrm{cum}\{y_m(t), y_{-m}^*(t), y_p^*(t), y_{-p}(t)\} \\
&= \sum_{k=1}^{K} c_{4,s_k} e^{j2m\omega_k}(e^{j2p\omega_k})^*, \quad m, p \in [-M, M]
\end{aligned} \tag{19}$$

Let $\bar{m} = m + M + 1$ and $\bar{p} = p + M + 1$, we define a special cumulant matrix $\mathbf{C}_1$, whose $(\bar{m}, \bar{p})$th element can be given as

$$\begin{aligned}
\mathbf{C}_1(\bar{m}, \bar{p}) &= \mathrm{cum}\{y_{\bar{m}-M-1}(t), y_{-\bar{m}+M+1}^*(t), \\
&\quad y_{\bar{p}-M-1}^*(t), y_{-\bar{p}+M+1}(t)\} \\
&= \sum_{k=1}^{K} c_{4,s_k} e^{j2(\bar{m}-M-1)\omega_k} \\
&\quad \times (e^{j2(\bar{p}-M-1)\omega_k})^*, \ \bar{m}, \bar{p} \in [1, 2M+1]
\end{aligned} \tag{20}$$

Obviously, the cumulant matrix $\mathbf{C}_1$ is only related to DOA parameters of mixed sources.

The cumulant matrix $\mathbf{C}_1$ can be expressed in a compact matrix form

$$\mathbf{C}_1 = \mathbf{B}\mathbf{C}_{4s}\mathbf{B}^H \tag{21}$$

where $\mathbf{C}_{4s} = \mathrm{diag}[c_{4,s_1}, c_{4,s_2}, \ldots, c_{4,s_K}]$, $\mathbf{B} = [\mathbf{b}(\theta_1), \ldots, \mathbf{b}(\theta_K)]$ can be regarded as the $(2M+1) \times K$ "virtual steering matrix", where

$$\begin{aligned}
\mathbf{b}(\theta_k) = \big[&e^{-j2M\omega_k}, e^{-j2(M-1)\omega_k}, \ldots, 1, \ldots, \\
&e^{j2(M-1)\omega_k}, e^{j2M\omega_k}\big]^T
\end{aligned} \tag{22}$$

is the $(2M+1) \times 1$ "virtual steering vector". Note that $\mathbf{b}(\theta_k)$ and $\mathbf{a}(\theta_k)$ have different phase difference between two adjacent elements.

According to near-field and far-field components, the cumulant matrix $\mathbf{C}_1$ can be expressed as

$$\begin{aligned}
\mathbf{C}_1 &= \mathbf{B}\mathbf{C}_{4s}\mathbf{B}^H = \mathbf{C}_N + \mathbf{C}_F \\
&= \mathbf{B}_N\mathbf{C}_{4s,N}\mathbf{B}_N^H + \mathbf{B}_F\mathbf{C}_{4s,F}\mathbf{B}_F^H
\end{aligned} \tag{23}$$

where $\mathbf{C}_N$ and $\mathbf{C}_F$ denote the near-field and far-field cumulant matrices. $\mathbf{B}_N = \left[\mathbf{b}(\theta_1), \ldots, \mathbf{b}(\theta_{K_1})\right]$ and $\mathbf{B}_F = \left[\mathbf{b}(\theta_{K_1+1}), \ldots, \mathbf{b}(\theta_K)\right]$ are the near-field and far-field virtual steering matrices, which corresponds to DOAs of near-field and far-field sources, respectively. $\mathbf{C}_{4s,\,N}$ and $\mathbf{C}_{4s,\,F}$ are given by

$$\mathbf{C}_{4s,N} = \mathrm{diag}[c_{4,s_1}, c_{4,s_2}, \ldots, c_{4,s_{K_1}}], \tag{24}$$

$$\mathbf{C}_{4s,F} = \mathrm{diag}[c_{4,s_{K_1+1}}, c_{4,s_{K_1+2}}, \ldots, c_{4,s_K}]. \tag{25}$$

As we all known, when the angular separation between two sources exceeds a certain value, the associated steering vectors are orthogonal or approximately orthogonal. Consider a ULA composed of 9 sensors $(M = 4)$ with a quarter-wavelength inter-element spacing, and one DOA is fixed at $\theta_j = 0^\circ$. Fig. 2 displays the value of Q_{jk} versus another DOA θ_k, where

$$Q_{jk} = \frac{|\mathbf{b}^H(\theta_j)\mathbf{b}(\theta_k)|}{2M+1} \tag{26}$$

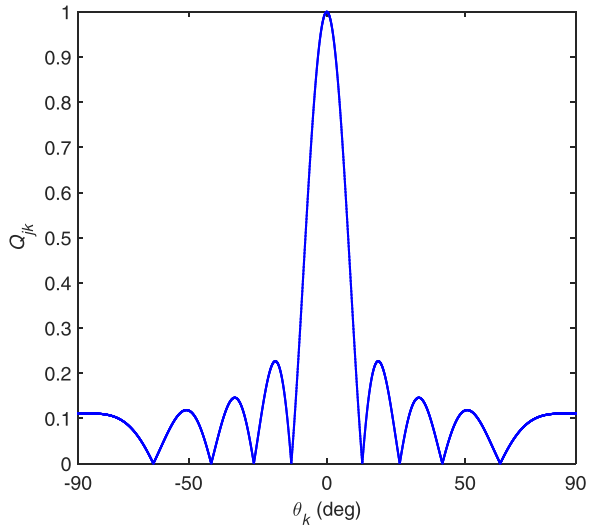

Fig. 2. The value of Q_{jk} versus θ_k. $\theta_j = 0^\circ$, $M = 4$.

is used to measure the orthogonality between $\mathbf{b}(\theta_j)$ and $\mathbf{b}(\theta_k)$. It can be seen from Fig. 2 that the value of Q_{jk} will become zero or at a very low level when the angular separation $|\theta_j - \theta_k|$ is greater than a certain value. That means $\mathbf{b}(\theta_j)$ and $\mathbf{b}(\theta_k)$ are orthogonal or approximately orthogonal. Based on the special property above, we can estimate the kurtosis of each signal.

The cumulant matrix $\mathbf{C}_1$ can be written as

$$\mathbf{C}_1 = \sum_{k=1}^{K} c_{4,s_k}\mathbf{b}(\theta_k)\mathbf{b}^H(\theta_k) \tag{27}$$

Pre-multiplying the above equation by $\mathbf{b}^H(\theta_j)$ ($j \in [1, K]$) and post-multiplying the above equation by $\mathbf{b}(\theta_j)$, we have

$$\mathbf{b}^H(\theta_j)\mathbf{C}_1\mathbf{b}(\theta_j) = \mathbf{b}^H(\theta_j)\left(\sum_{k=1}^{K} c_{4,s_k}\mathbf{b}(\theta_k)\mathbf{b}^H(\theta_k)\right)\mathbf{b}(\theta_j) \tag{28}$$

Here we assume that all signals impinge on the receiver array from distinct directions, so that any two of the associated steering vectors are orthogonal ($\mathbf{b}^H(\theta_j)\mathbf{b}(\theta_k) = 0,\ j \neq k$), or approximately orthogonal ($\mathbf{b}^H(\theta_j)\mathbf{b}(\theta_k) \ll \mathbf{b}^H(\theta_j)\mathbf{b}(\theta_j),\ j \neq k$). Then the remaining terms excluding $c_{4,s_k}\mathbf{b}^H(\theta_k)\mathbf{b}(\theta_k)\mathbf{b}^H(\theta_k)\mathbf{b}(\theta_k)$ ($j = k$) in (28) can be neglected, resulting in

$$\mathbf{b}^H(\theta_k)\mathbf{C}_1\mathbf{b}(\theta_k) = c_{4,s_k}\mathbf{b}^H(\theta_k)\mathbf{b}(\theta_k)\mathbf{b}^H(\theta_k)\mathbf{b}(\theta_k). \tag{29}$$

Thus, the kurtosis of the kth signal can be given by

$$c_{4,s_k} = \frac{\mathbf{b}^H(\theta_k)\mathbf{C}_1\mathbf{b}(\theta_k)}{|\mathbf{b}^H(\theta_k)\mathbf{b}(\theta_k)|^2}. \tag{30}$$

With the far-field DOA estimates $\{\hat{\theta}_k,\ k = K_1 + 1, \ldots, K\}$, substituting $\hat{\theta}_k$ into (30), we can estimate the kurtosis of each far-field signal by

$$\hat{c}_{4,s_k} = \frac{\mathbf{b}^H(\hat{\theta}_k)\mathbf{C}_1\mathbf{b}(\hat{\theta}_k)}{|\mathbf{b}^H(\hat{\theta}_k)\mathbf{b}(\hat{\theta}_k)|^2}, \quad k \in [K_1 + 1, K]. \tag{31}$$

Then, the far-field cumulant matrix $\mathbf{C}_F$ can be estimated as

$$\hat{\mathbf{C}}_F = \hat{\mathbf{B}}_F\hat{\mathbf{C}}_{4s,F}\hat{\mathbf{B}}_F^H \tag{32}$$

where

$$\hat{\mathbf{B}}_F = [\mathbf{b}(\hat{\theta}_{K_1+1}), \ldots, \mathbf{b}(\hat{\theta}_K)], \tag{33}$$

$$\hat{\mathbf{C}}_{4s,F} = \mathrm{diag}[\hat{c}_{4,s_{K_1+1}}, \hat{c}_{4,s_{K_1+2}}, \ldots, \hat{c}_{4,s_K}]. \tag{34}$$

Further, the near-field cumulant matrix $\mathbf{C}_N$ can be estimated by

$$\hat{\mathbf{C}}_N = \mathbf{C}_1 - \hat{\mathbf{C}}_F \tag{35}$$

It can be seen that the far-field components have been effectively removed in (35), and a more reasonable classification of the signal types can be achieved.

Implementing the EVD of $\hat{\mathbf{C}}_N$ as follows:

$$\hat{\mathbf{C}}_N = \mathbf{E}_s\mathbf{\Lambda}_s\mathbf{E}_s^H + \mathbf{E}_n\mathbf{\Lambda}_n\mathbf{E}_n^H \tag{36}$$

where $\mathbf{\Lambda}_s$ is the $K_1 \times K_1$ diagonal matrix containing the K_1 largest eigenvalues of $\hat{\mathbf{C}}_N$, and $\mathbf{E}_s$ is the $(2M+1) \times K_1$ signal-subspace matrix spanned by the eigenvectors corresponding to the K_1 largest eigenvalues. $\mathbf{\Lambda}_n$ is the $(2M+1-K_1) \times (2M+1-K_1)$ diagonal matrix containing the $2M+1-K_1$ smallest eigenvalues of $\hat{\mathbf{C}}_N$, and $\mathbf{E}_n$ is the $(2M+1) \times (2M+1-K_1)$ noise-subspace matrix spanned by the eigenvectors related to the $2M+1-K_1$ smallest eigenvalues.

The DOAs of near-field sources can be obtained by finding the K_1 peaks from the following DOA spectrum

$$P_N(\theta) = \left[\mathbf{a}^H(\theta)\mathbf{E}_n\mathbf{E}_n^H\mathbf{a}(\theta)\right]^{-1}. \tag{37}$$

3.3. Range estimations of near-field sources

With the near-field DOA estimates $\{\hat{\theta}_k,\ k = 1, \ldots, K_1\}$, the range estimations of near-field sources can be performed by substituting each $\hat{\theta}_k$ into the following spectral function

$$g(\theta, r) = \left[\mathbf{a}^H(\theta, r)\mathbf{U}_n\mathbf{U}_n^H\mathbf{a}(\theta, r)\right]^{-1} \tag{38}$$

The range estimate of the kth source is given by

$$\hat{r}_k = \min_r g(\hat{\theta}_k, r), \quad k \in [1, K_1] \tag{39}$$

It is noteworthy that $\hat{\theta}_k$ and $\hat{r}_k$ achieve automatic pairing without any extra processing.

3.4. Implementation of proposed algorithm

Based on the above description, the implementation of the proposed algorithm for locating mixed source with N snapshot data can be summarized as follows:

Step 1) Calculate the sample covariance matrix $\hat{\mathbf{R}} = (1/N)\sum_{t=1}^{N}\mathbf{y}(t)\mathbf{y}^H(t)$, and eigendecompose $\hat{\mathbf{R}}$ to obtain the noise-subspace matrix $\mathbf{U}_n$.

Step 2) Create the far-field DOA spectrum $P_F(\theta)$ (17), and estimate the DOAs of far-field sources by 1-D search.

Step 3) Calculate the sample cumulant matrix $\hat{\mathbf{C}}_1$ of N snapshot data, and estimate the kurtosis of far-field signals by (31), and then estimate the far-field cumulant matrix $\mathbf{C}_F$ via (32).

Step 4) Obtain the estimate of near-field cumulant matrix $\mathbf{C}_N$ using (35), and eigendecompose $\hat{\mathbf{C}}_N$ to obtain the noise-subspace matrix $\mathbf{E}_n$.

Step 5) Create the near-field DOA spectrum $P_N(\theta)$ (37), and estimate the DOAs of near-field sources by 1-D search.

Step 6) Substitute each $\hat{\theta}_k$ into the spectral function (38), and estimate the ranges of near-field sources through (39).

4. Simulation results

In this section, several simulation examples are provided to verify the performance of the proposed approach as well as perform a comparison with the TSMUSIC method [21], the MBODS method [22] and the related Cramer-Rao lower bound (CRLB) [22]. In all examples, a nine-element ULA with inter-element spacing $d = \lambda/4$ is considered. The input signal-to-noise ratio (SNR) of the kth signal is defined $10\log_{10}(\sigma_k^2/\sigma_n^2)$. Assume that all incident sources have equal power and the number of sources is known. The results shown below are evaluated by the estimated root mean square error (RMSE) from the average results of $M_C = 500$ independent Monte Carlo simulations, where the RMSE is defined as

$$\mathrm{RMSE}(\alpha_k) = \sqrt{\frac{1}{M_C}\sum_{j=1}^{M_C}\left(\hat{\alpha}_k^{(j)} - \alpha_k\right)^2} \tag{40}$$

where α_k denotes the DOA θ_k or the range r_k, and $\hat{\alpha}_k^{(j)}$ is the estimate of α_k for the jth independent trial respectively.

In the first example, we consider the mixed sources scenario with one far-field source and one near-field source, which are located at $(-45^\circ, 2.7\lambda)$ and $(5^\circ, \infty)$, respectively. The SNR varies from -5 dB to 30 dB, and the number of snapshots is set to $N = 400$. Figs. 3a and b respectively demonstrate the RMSEs of DOA and range estimations using the proposed method. Furthermore, the RMSEs of the TSMUSIC method, the MBODS method, and

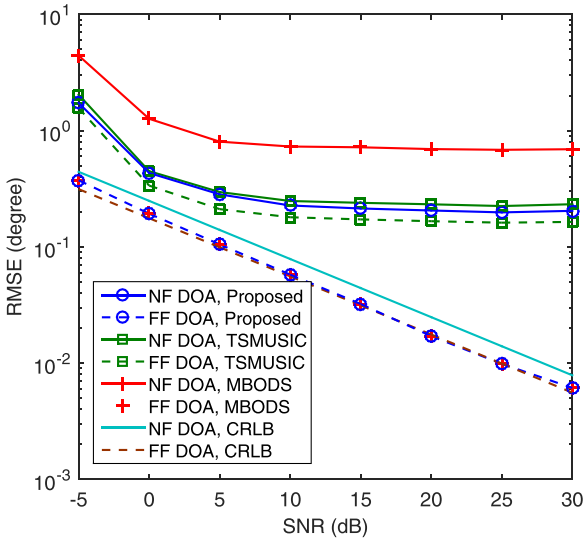

(a)

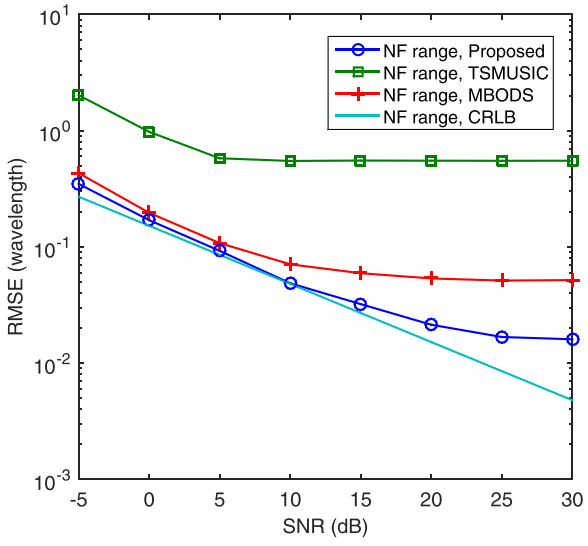

(b)

Fig. 3. RMSEs of DOA and range estimations for one near-field and one far-field sources versus the SNR. $\theta_1 = -45^\circ$, $r_1 = 2.7\lambda$, $\theta_2 = 5^\circ$, $r_2 = \infty$, $N = 400$ snapshots, 500 independent simulations. (a) DOA estimation. (b) Range estimation.

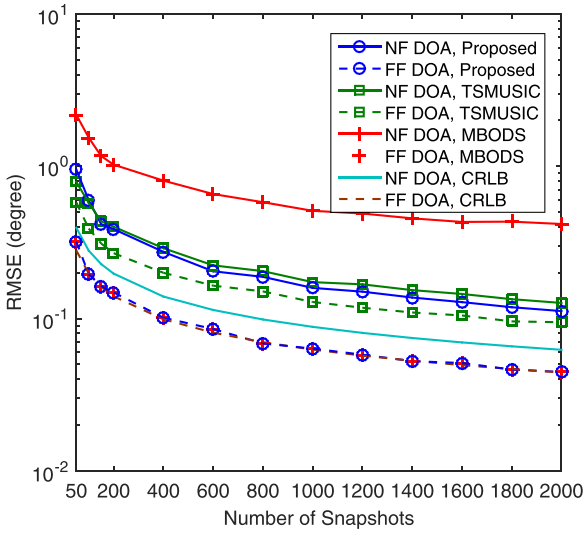

(a)

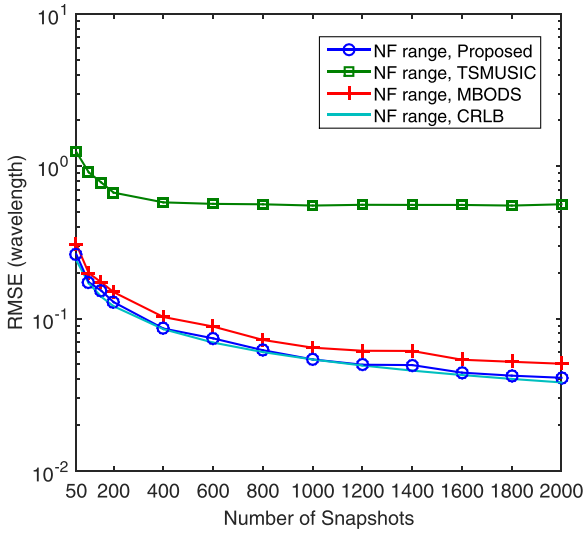

(b)

Fig. 4. RMSEs of DOA and range estimations for one near-field and one far-field sources versus the number of snapshots. $\theta_1 = -45^\circ$, $r_1 = 2.7\lambda$, $\theta_2 = 5^\circ$, $r_2 = \infty$, SNR = 5 dB, 500 independent simulations. (a) DOA estimation. (b) Range estimation.

the CRLB are also presented for comparison. As seen from those figures, the proposed method and the TSMUSIC method achieve similar performance for DOA estimations of near-field sources, and both of them perform evidently better than the MBODS method. For DOA estimations of far-field sources, the proposed method and the MBODS method have the same performance, they all outperform the TSMUSIC method obviously and their performances are close to the CRLB across a wide range of SNR. For range estimations of near-field sources, the proposed method is obviously better than the TSMUSIC method, and it also outperforms the MBODS method at high SNRs. Hence, the proposed method achieves better localization performance than TSMUSIC and MBODS in the near-field sources scenario. That is because our approach makes a more reasonable classification of the source types after acquiring the DOAs of far-field sources.

In the second example, we assess the performance of the proposed algorithm in terms of the number of snapshots. The number of snapshots is varied from 50 to 2000, and the SNR is equal to 5 dB, while the other simulation parameters are the same as those in the first example. The RMSEs of DOA and range estimations for the proposed algorithm are respectively shown in Figs. 4a and b, compared with those of the TSMUSIC method, the MBODS method, and the CRLB. It can be observed from Figs. 4a and b that the simulation results are similar to those of the first example. For DOA estimations of near-field sources, the proposed method acquires much higher precision than the MBODS method, while it is superior to the TSMUSIC method for DOA estimations of far-field sources. For range estimations of near-field sources, the proposed approach outperforms both TSMUSIC and MBODS, and its performance is very close to the CRLB across a wide range of snapshot

number. Furthermore, all performance curves become stabilized as the number of snapshots increases.

5. Conclusions

This paper has presented a novel localization algorithm for scenarios where both near-field and far-field sources may exist simultaneously. The presented algorithm implements DOA and range estimations by using second-order statistics together with fourth-order statistics. It does not require 2-D spectral search or extra parameter pairing processing. Compared with some existing techniques such as TSMUSIC and MBODS, our approach can make a more reasonable classification of the source types and exhibit an improved localization accuracy of near-field sources. Simulation results verify the performance of the proposed algorithm.

Acknowledgment

This work is supported by the National Natural Science Foundation of China under Grants 61301155 and 61571081, the 111 project (B14039), and the Fundamental Research Funds for the Central Universities of China under Grant ZYGX2016J008.

References

[1] H. Krim, M. Viberg, Two decades of array signal processing research: the parametric approach, IEEE Signal Process. Mag. 13 (4) (1996) 67–94.
[2] M.N.E. Korso, R. Boyer, A. Renaux, S. Marcos, Conditional and unconditional cramér–rao bounds for near-field source localization, IEEE Trans. Signal Process. 58 (5) (2010) 2901–2907.
[3] M.N.E. Korso, R. Boyer, A. Renaux, S. Marcos, Statistical analysis of achievable resolution limit in the near field source localization context, Signal Process. 92 (2) (2012) 547–552.
[4] J.P. Delmas, M.N.E. Korso, H. Gazzah, M. Castella, CRB analysis of planar antenna arrays for optimizing near-field source localization, Signal Process. 127 (2016) 117–134.
[5] R. Schmidt, Multiple emitter location and signal parameter estimation, IEEE Trans. Antennas Propag. 34 (3) (1986) 276–280.
[6] R. Roy, T. Kailath, ESPRIT-estimation of signal parameters via rotational invariance techniques, IEEE Trans. Acoust. Speech Signal Process. 37 (7) (1989) 984–995.
[7] Y.-D. Huang, M. Barkat, Near-field multiple source localization by passive sensor array, IEEE Trans. Antennas Propag. 39 (7) (1991) 968–975.
[8] A. Weiss, B. Friedlander, Range and bearing estimation using polynomial rooting, IEEE J. Ocean. Eng. 18 (2) (1993) 130–137.
[9] D. Starer, A. Nehorai, Passive localization of near-field sources by path following, IEEE Trans. Signal Process. 42 (3) (1994) 677–680.
[10] J.-H. Lee, Y.-M. Chen, C.-C. Yeh, A covariance approximation method for near–field direction-finding using a uniform linear array, IEEE Trans. Signal Process. 43 (5) (1995) 1293–1298.
[11] R.N. Challa, S. Shamsunder, High-order subspace-based algorithms for passive localization of near-field sources, in: Proc. 29th Asilomar Conf. Signals, Syst., Comput., volume 2, Pacific Grove, CA, 1995, pp. 777–781.
[12] E. Grosicki, K. Abed-Meraim, Y. Hua, A weighted linear prediction method for near-field source localization, IEEE Trans. Signal Process. 53 (10) (2005) 3651–3660.
[13] Y. Wu, L. Ma, C. Hou, G. Zhang, J. Li, Subspace-based method for joint range and DOA estimation of multiple near-field sources, Signal Process. 86 (8) (2006) 2129–2133.
[14] W. Zhi, M.Y.-W. Chia, Near-field source localization via symmetric subarrays, IEEE Signal Process. Lett. 14 (6) (2007) 409–412.
[15] W.-J. Zeng, X.-L. Li, H. Zou, X.-D. Zhang, Near-field multiple source localization using joint diagonalization, Signal Process. 89 (2) (2009) 232–238.
[16] J. Liang, X. Zeng, B. Ji, J. Zhang, F. Zhao, A computationally efficient algorithm for joint range–DOA–frequency estimation of near-field sources, Digital Signal Process. 19 (4) (2009) 596–611.
[17] J. Liang, D. Liu, Passive localization of near-field sources using cumulant, IEEE Sensors J. 9 (8) (2009) 953–960.
[18] J.A. Chaaya, J. Picheral, S. Marcos, Localization of spatially distributed near–field sources with unknown angular spread shape, Signal Process. 106 (2015) 259–265.
[19] J. Xie, H. Tao, X. Rao, J. Su, Efficient method of passive localization for near-field noncircular sources, IEEE Antennas Wireless Propag. Lett. 14 (2015) 1223–1226.
[20] L. Jianzhong, Y. Wang, W. Gang, Signal reconstruction for near-field source localisation, IET Signal Process. 9 (3) (2015) 201–205.
[21] J. Liang, D. Liu, Passive localization of mixed near-field and far-field sources using two-stage MUSIC algorithm, IEEE Trans. Signal Process. 58 (1) (2010) 108–120.
[22] J. He, M. Swamy, M.O. Ahmad, Efficient application of MUSIC algorithm under the coexistence of far-field and near-field sources, IEEE Trans. Signal Process. 60 (4) (2012) 2066–2070.
[23] G. Liu, X. Sun, Efficient method of passive localization for mixed far-field and near-field sources, IEEE Antennas Wireless Propag. Lett. 12 (2013) 902–905.
[24] B. Wang, Y. Zhao, J. Liu, Mixed-order MUSIC algorithm for localization of far–field and near-field sources, IEEE Signal Process. Lett. 20 (4) (2013) 311–314.
[25] J.-J. Jiang, F.-J. Duan, J. Chen, Y.-C. Li, X.-N. Hua, Mixed near-field and far-field sources localization using the uniform linear sensor array, IEEE Sensors J. 13 (8) (2013) 3136–3143.
[26] B. Wang, J. Liu, X. Sun, Mixed sources localization based on sparse signal reconstruction, IEEE Signal Process. Lett. 19 (8) (2012) 487–490.
[27] Y. Tian, X. Sun, Mixed sources localisation using a sparse representation of cumulant vectors, IET Signal Process. 8 (6) (2014) 606–611.
[28] G. Liu, X. Sun, Y. Liu, Y. Qin, Low-complexity estimation of signal parameters via rotational invariance techniques algorithm for mixed far-field and near-field cyclostationary sources localisation, IET Signal Process. 7 (5) (2013) 382–388.
[29] K. Wang, L. Wang, J.-R. Shang, X.-X. Qu, Mixed near-field and far-field source localization based on uniform linear array partition, IEEE Sensors J. 16 (22) (2016) 8083–8090.
[30] G. Liu, X. Sun, Two-stage matrix differencing algorithm for mixed far-field and near-field sources classification and localization, IEEE Sensors J. 14 (6) (2014) 1957–1965.
[31] G. Liu, X. Sun, Spatial differencing method for mixed far-field and near-field sources localization, IEEE Signal Process. Lett. 21 (11) (2014) 1331–1335.
[32] M. Wax, T. Kailath, Detection of signals by information theoretic criteria, IEEE Trans. Acoust. Speech Signal Process. ASSP-33 (2) (1985) 387–392.